Vehicle State and Parameter Estimation Based on Dual Unscented Particle Filter Algorithm

Lin Fen(林棻)*, *Wang Hao*(王浩), *Wang Wei*(王伟), *Liu Cunxing*(刘存星), *Xie Chunli*(谢春利)

College of Energy and Power Engineering, Nanjing University of Aeronautics and Astronautics, Nanjing, 210016, P. R. China

(Received 4 November 2013; revised 24 December 2013; accepted 25 December 2013)

Abstract: Acquisition of real-time and accurate vehicle state and parameter information is critical to the research of vehicle dynamic control system. By studying the defects of the former Kalman filter based estimation method, a new estimating method is proposed. First the nonlinear vehicle dynamics system, containing inaccurate model parameters and constant noise, is established. Then a dual unscented particle filter (DUPF) algorithm is proposed. In the algorithm two unscented particle filters run in parallel, states estimation and parameters estimation update each other. The results of simulation and vehicle ground testing indicate that the DUPF algorithm has higher state estimation accuracy than unscented Kalman filter (UKF) and dual extended Kalman filter (DEKF), and it also has good capability to revise model parameters.

Key words: vehicle dynamics; dual unscented particle filter (DUPF); state estimation; virtual experiment

CLC number: U461.6 **Document code**: A **Article ID**: 1005-1120(2014)05-0568-08

1 Introduction

A lack of information of vehicle states and parameters presents a major obstacle for the development of vehicle control systems. The effectiveness of vehicle stability control mainly depends on the accuracy of vehicle states and parameters, especially the side slip angle and yaw rate. Currently yaw rate can already be measured by gyro. However, information of side slip angle has to be acquired through complicated method such as state estimation and GPS positioning. Among the above two methods, state estimation is easier and more economical than the GPS method[1]. Though some states can be measured by sensors directly, state estimation method is also able to dramatically reduce the interference brought by the measurement noise and process noise contained in the signal.

Currently vehicle state estimation methods are general Kalman filter (KF)[2], extended Kalman filter (EKF)[3] and its improved algorithms[4-5], unscented Kalman filter (UKF)[6], particle filter (PF)[7], neural network method[8], state observer method[9] and fuzzy logic method[10], etc. These methods all estimate the critical control variables of vehicle control system, including side-slip angle, lateral velocity and yaw rate. They are all "model based estimator". In these estimators, vehicle parameters such as mass, moment of inertia, and center of mass position, are all assumed invariant and measured approximately. However, these parameters may vary with different working condition when driving. For instance, difference between an empty and a full load heavy truck's influence to the cen-

Foundation items: Supported by the National Natural Science Foundation of China (10902049); the Chinese Postdoctoral Science Foundation (2012M521073); the Fundamental Research Funds for the Central Universities; the Jiangsu Planned Projects for Postdoctoral Research Funds (1302020C); the Nanjing University of Aeronautics and Astronautics Student Innovative Training Program (20120119101535); the Fundation of Graduate Innovation Center in Nanjing University of Aeronautics and Astronautics (kfjj201404).

* **Corresponding author**: Lin Fen, Associate Professor, E-mail: flin@nuaa.edu.cn.

ter of mass position and moment of inertia is obvious. Therefore, it is essential to consider the uncertainty of parameters when estimating the vehicle states. During the vehicle state estimation process, updating the uncertain vehicle parameters simultaneously is the only way to obtain more accurate driving information.

With regarding to various control logic requirements of vehicle dynamic control system, a multi-states estimation method of running vehicle is proposed by applying the newly developed dual unscented particle filter (DUPF) algorithm in vehicle dynamics estimation.

2 Non-linear Vehicle Dynamic Model

2.1 Full vehicle model

As shown in Fig. 1, the proposed estimation method is a 7-DOF non-linear vehicle dynamic model which represents lateral, longitudinal, yaw motion of a vehicle and the rotating motion of the four tires.

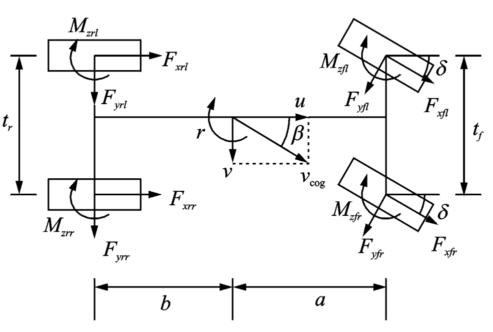

Fig. 1 7-DOF non-linear vehicle dynamic model

The equations of vehicle motion are written as:

Longitudinal

$$\dot{u} = a_x + vr \tag{1}$$

$$a_x = (F_{xfl}\cos\delta + F_{xfr}\cos\delta + F_{xrl} + F_{xrr} - F_{yfl}\sin\delta - F_{yfr}\sin\delta)/m \tag{2}$$

Lateral

$$\dot{v} = a_y - ur \tag{3}$$

$$a_y = (F_{xfl}\sin\delta + F_{xfr}\sin\delta + F_{yfl}\cos\delta + F_{yfr}\cos\delta + F_{yrl} + F_{yrr})/m \tag{4}$$

Yaw

$$\Gamma = \frac{t_f}{2}F'_{xfl} - \frac{t_f}{2}F'_{xfr} + \frac{t_r}{2}F_{xrl} - \frac{t_r}{2}F_{xrr} + aF'_{yfl} + aF'_{yfr} - bF_{yrl} - bF_{yrr} + M_{zfl} + M_{zfr} + M_{zrl} + M_{zrr} \tag{5}$$

$$\dot{r} = \frac{\Gamma}{I_z} \tag{6}$$

where $F'_{xij} = F_{xij}\cos\delta - F_{yij}\sin\delta$

$F'_{yij} = F_{yij}\cos\delta + F_{xij}\sin\delta$

where $\dot{u}$ represents the longitudinal velocity, $\dot{v}$ the lateral velocity, a_x the longitudinal acceleration, a_y the lateral acceleration, $\dot{r}$ the yaw rate, β the vehicle sideslip angle, Γ the yaw moment on z axis, δ the steering angle of front tire, F_{xij} the longitudinal force of each tire, F_{yij} the lateral force of each tire, M_{zij} the self-aligning torque of each tire, m the vehicle mass, I_z the vehicle moment of inertia on z axis, a, b are the distances between the center of gravity to the front and the rear axle, respectively.

Solving vertical load, slip angle and slip of each tire involvomg with the rotational motion can be found in Ref. [11]. Here we will not go into details of them.

2.2 Tire model

Pacejka non-linear tire model[12] is applied. The input variables of this model are vertical load, slip angle, tire slip.

Lateral force, longitudinal force and self-aligning torque of each tire can be calculated from unified Eqs. (7−9).

$$y(x) = D\sin(C\arctan(Bx - E(Bx - \arctan Bx))) \tag{7}$$

$$Y(X) = y(x) + s_v \tag{8}$$

$$x = X + s_h \tag{9}$$

where the output variable Y in Eq. (8) represents tire side force F_x, tire longitudinal force F_y and tire self-aligning torque M_z in different cases. The input variable X in Eq. (9) represents the tire slip S (when calculating longitudinal force) and tire sideslip angle α (when calculating lateral and self-aligning torque). Detailed expressions of parameters B, C, D, E, s_v, s_h in Eq. (7) see Ref. [12]. In the paper, under vertical load of 3.16 kN, the related parameters of tire model are valued as $B = 0.237$, $C = 1.65$, $I_z = 3\ 610.5$, $E = 0.707$, $s_v = 40.379$, $s_h = 0.047\ 3$.

2.3 Noise contained non-linear vehicle system

State vector of non-linear vehicle system is written as

$$\boldsymbol{x}^s = [u, v, a_x, a_y, r, \beta, \Gamma]^T \tag{10}$$

Parameter vector of non-linear vehicle system is written as

$$\boldsymbol{x}^{\mathrm{p}}=[m, I_z, a]^{\mathrm{T}} \tag{11}$$

Input of system is

$$\boldsymbol{u}=[\delta, \omega_{fl}, \omega_{fr}, \omega_{rl}, \omega_{rr}]^{\mathrm{T}} \tag{12}$$

Observation vector is

$$\boldsymbol{y}=[r, a_y, u]^{\mathrm{T}} \tag{13}$$

In the state estimation, process noise is set as a zero-mean white Gaussian noise sequence, and the covariance matrix is given by

$$\boldsymbol{Q}=0.01 \cdot |\max(\mathrm{state}(i))-\min(\mathrm{state}(i))| \quad i=1,\cdots,7;0 \leqslant t \leqslant 10 \tag{14}$$

where max(state(i)) are min(state(i)) are the maximum and the minimum values of the ith state parameter during the whole period, respectively.

Covariance matrix of measurement noise is set as a zero-mean white Gaussian noise sequence, and the covariance matrix is given by

$$\boldsymbol{R}=0.05 \cdot |\max(y(i))-\min(y(i))| \quad i=1,\cdots,3;0 \leqslant t \leqslant 10 \tag{15}$$

where max($y(i)$) and min($y(i)$) are the maximum and the minimum valus of the ith measurement parameter through the whole period, respectively.

3 Estimation Method Based on DUPF Algorithm

Based on the unscented particle filter (UPF)[7], DUPF is proposed.

3.1 PF algorithm

PF is another type of non-linear estimation method compared with various Kalman filter based algorithm. PF demonstrates distinct advantages towards non-linear estimation[13]. The core concept of PF is using the weighted sum of a series of random samples to represent posterior probability density. PF algorithm is given as follows[7]:

(1) Initialization

Extract N particles from the prior distribution $p(x_0)$.

$x_0(i) \quad i=1,2,\cdots,N$

(2)Importance sampling

Extract $x_k(i)$—$q(x_k|x_{0:k-1}(i), y_{1:k}), i=1,2,\cdots,N$

Calculate weights of the new samples

$$W_k(i)=W_{k-1}(i)\frac{p(y_k \mid x_k(i))p(x_k \mid x_{k-1}(i))}{q(x_k(i) \mid x_{0:k-1}(i), y_{1:k})} \quad i=1,2,\cdots,N \tag{16}$$

Normalize the weights

$$W_k(i)=\frac{W_k^*(i)}{\sum_{i=1}^{N} W_k^*(i)} \tag{17}$$

(3) Resample

Randomly extract a sample u—$U[0,1]$ in every step. Particles $x_k(i)$ which meet the following equation will be selected and duplicated to the new set of particles. Meanwhile, weights of all particles are set as $1/N$.

$$\sum_{j=1}^{i-1} W_k(j) \leqslant u \leqslant \sum_{j=1}^{i} W_k(j) \tag{18}$$

(4) Filter output

The MMSE estimation of x_k is given by

$$\hat{x}_k=\sum_{i=1}^{N} W_k(i) x_k(i) \tag{19}$$

3.2 DUPF algorithm

Two UPF run parallel in DUPF. State estimation is followed with parameter estimation. State estimation is integrated between parameter prediction process and correction process. System states and parameters are able to be estimated in real-time. In order to resolve two major drawbacks, namely sampling blindness and particle degeneration, lies in PF, DUPF adopts certain sampling strategy. Through Unscented Transformation (UT), an importance function $q(x_k \mid x_{0:k-1}(i), y_{1:k})$ better than the generic PF is acquired to eliminate particle degeneration. Meanwhile, the latest observation values of the system are utilized in this algorithm; hence the estimation precision is improved.

Generally, state and observation equations of non-linear discrete system are described as Eq. (20,21), respectively

$$\boldsymbol{x}_{k+1}^{\mathrm{s}}=f(\boldsymbol{x}_k^{\mathrm{s}}, \boldsymbol{u}_k, \boldsymbol{x}_k^{\mathrm{p}})+w_k \tag{20}$$

$$\boldsymbol{y}_k=h(\boldsymbol{x}_k^{\mathrm{s}}, \boldsymbol{x}_k^{\mathrm{p}})+v_k \tag{21}$$

where $\boldsymbol{x}^{\mathrm{s}}$ is the state vector, $\boldsymbol{x}^{\mathrm{p}}$ the parameter vector, $\boldsymbol{u}$ the system input, $\boldsymbol{y}$ the is observation vector, w and v are process noise and measurement noise, respectively.

First, calculate the sigma points

$$\chi_{k-1}^{i}=[\bar{x}_{k-1}^{i} \quad \bar{x}_{k-1}^{i}+\sqrt{(n+\lambda)P_{k-1}^{i}} \quad \bar{x}_{k-1}^{i}-\sqrt{(n+\lambda)P_{k-1}^{i}}]$$

Parameter estimation

Time update

$$\chi_{k|k-1}^{\mathrm{p},i}=\chi_{k-1|k-1}^{\mathrm{p},i} \tag{22}$$

$$P_{p_{k|k-1}}^{i}=P_{p_{k-1|k-1}}^{i}+R_{k-1} \tag{23}$$

$$D_{k|k-1}^{i}=h(\hat{x}_{k-1|k-1}^{\mathrm{s}},\chi_{k|k-1}^{\mathrm{p},i},k) \tag{24}$$

$$\hat{d}_{k|k-1}^{i}=\sum_{j=0}^{2n}W_{j}^{\mathrm{p}}D_{j,k|k-1}^{i} \tag{25}$$

Measurement update

$$P_{d_k d_k}^{i}=\sum_{j=0}^{2n}W_{j}^{c}(D_{j,k|k-1}^{i}-\hat{d}_{k}^{i})(D_{j,k|k-1}^{i}-\hat{d}_{k}^{i})^{\mathrm{T}}+R \tag{26}$$

$$P_{x_k^{\mathrm{p}}d_k}^{i}=\sum_{j=0}^{2n}W_{j}^{c}(\chi_{j,k|k-1}^{\mathrm{p},i}-x_{k}^{\mathrm{p},i})(D_{j,k|k-1}^{i}-d_{k}^{i})^{\mathrm{T}} \tag{27}$$

$$K_{k}^{\mathrm{p},i}=P_{x_k^{\mathrm{p}}d_k}^{i}P_{d_k d_k}^{i}{}^{-1} \tag{28}$$

$$\hat{x}_{k}^{\mathrm{p},i}=\hat{x}_{k|k-1}^{\mathrm{p},i}+K_{k}^{\mathrm{p},i}(d_{k}-\hat{d}_{k|k-1}^{i}) \tag{29}$$

$$P_{k}^{i}=P_{k|k-1}^{i}-K_{k}^{i}P_{y_k y_k}K_{k}^{i\mathrm{T}} \tag{30}$$

All remaining steps in UPF remain the same with those in the PF Eqs. (16—19).

State estimation

Time update

$$\chi_{k|k-1}^{\mathrm{s},i}=f(\chi_{k-1}^{\mathrm{s},i},u_{k-1},x_{k-1}^{p}) \tag{31}$$

$$\hat{x}_{k|k-1}^{\mathrm{s},i}=\sum_{j=0}^{2n}W_{j}^{m}\chi_{j,k|k-1}^{\mathrm{s},i} \tag{32}$$

$$P_{k|k-1}^{\mathrm{s},i}=\sum_{j=0}^{2n}W_{j}^{c}\chi_{j,k|k-1}^{\mathrm{s},i} \tag{33}$$

$$\psi_{k|k-1}^{i}=h(\chi_{k|k-1}^{s,i},x_{k|k-1}^{\mathrm{s},i}) \tag{34}$$

$$y_{k|k-1}^{i}=\sum_{j=0}^{2n}W_{j}^{m}\psi_{j,k|k-1}^{i} \tag{35}$$

Measurement update

$$P_{y_k y_k}^{i}=\sum_{j=0}^{2n}W_{j}^{c}(\psi_{j,k|k-1}^{i}-\hat{y}_{k|k-1}^{i})(\psi_{j,k|k-1}^{i}-\hat{y}_{k|k-1}^{i})^{\mathrm{T}} \tag{36}$$

$$P_{x_k^{\mathrm{s}}y_k}^{i}=\sum_{j=0}^{2n}W_{j}^{c}(\chi_{j,k|k-1}^{\mathrm{s},i}-\hat{x}_{k|k-1}^{\mathrm{s},i})(\psi_{j,k|k-1}^{i}-\hat{y}_{k|k-1}^{i})^{\mathrm{T}} \tag{37}$$

$$K_{k}^{i}=P_{x_k^{\mathrm{s}}y_k}^{i}(P_{y_k y_k}^{i})^{-1} \tag{38}$$

$$\hat{x}_{k}^{\mathrm{s},i}=\hat{x}_{k|k-1}^{\mathrm{s},i}+K_{k}^{i}(y_{k}-y_{k|k-1}^{i}) \tag{39}$$

$$P_{k}^{i}=P_{k|k-1}^{i}-K_{k}^{i}P_{y_k y_k}K_{k}^{i\mathrm{T}} \tag{40}$$

All remaining steps in the UPF remain the same with the PF Eqs. (16—19).

4 Experimental Verification Based on ADAMS

A virtual experiment is conducted on ADAMS to verify the proposed algorithm. Parameters of the vehicle is: $m=1\,528$ kg, $a=1.48$ m, $b=1.08$ m, the height of center of gravity (CoG) $h=0.432$ m, $I_z=2\,440$ kg • m^2, the width of front track $t_{\mathrm{f}}=1.52$ m, the width of rear track $t_{\mathrm{r}}=1.594$ m, the effective rolling radius of wheel $r_e=0.33$ m.

ADAMS full vehicle model is composed of front and rear suspension subsystem, body subsystem, steering subsystem, braking subsystem, front and rear tire subsystems. Establish input and output "Communicator" between subsystems. Tire model is the Pac89 tire model contained in the ADAMS software. The assembled ADAMS vehicle model is shown in Fig. 2.

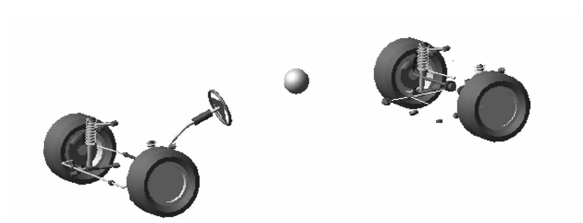

Fig. 2 ADAMS vehicle model

Requested vehicle driving route is generated to simulate the vehicle control response under extreme condition in ADAMS. Vehicle is driven along the route shown in Fig. 3. The whole operation period is 10 s, sampling time is 0.01 s.

To inspect the estimation performance of

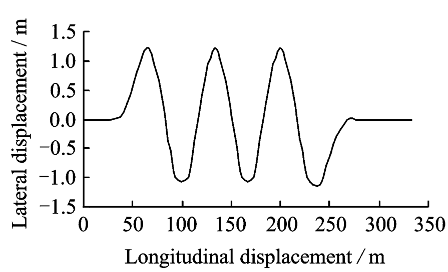

Fig. 3 Serpentine route

DUPF algorithm on the non-linear vehicle system, this work compares the DUPF algorithm with other two estimation algorithms, namely UKF and dual extend Kalman filter (DEKF)[7]. The initial vehicle parameters of all the three algorithms are inaccurate, set $m_0=1\ 250$ kg, $I_{z0}=2\ 100$ kg·m^2, $a_0=1.25$ m. As DUPF and DEKF algorithms have the capability of parameter adaptation, the vehicle parameters in these two algorithms are adjusting online.

Fig. 4 is a comparison between the estimated and experimental value of six key state parameters u, v, a_x, a_y, r, β.

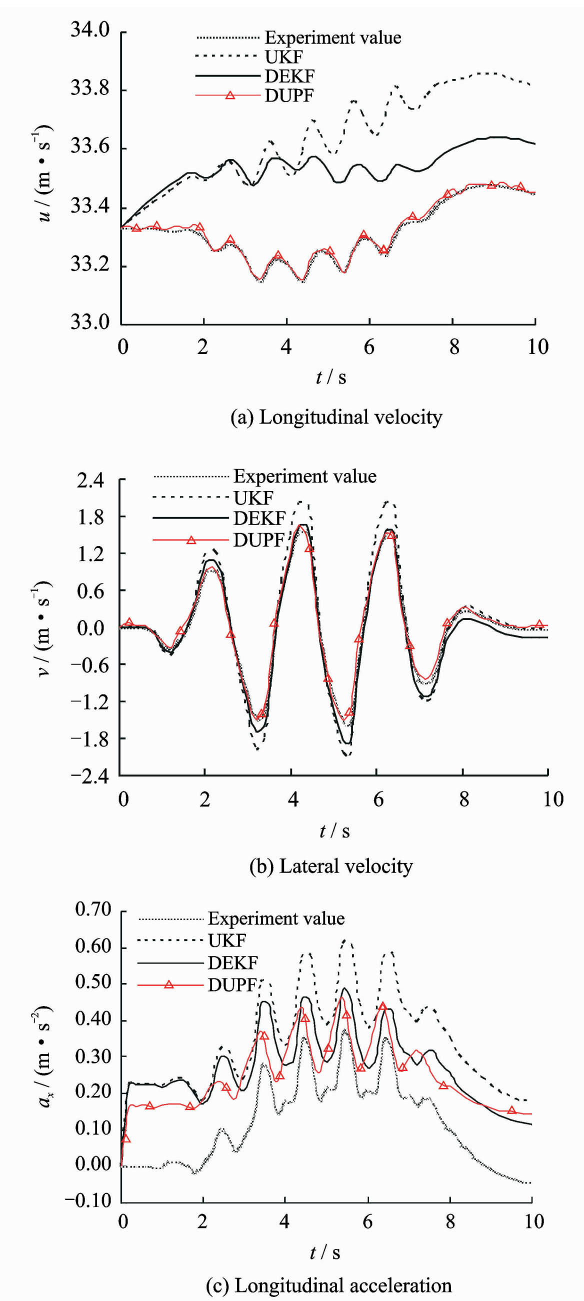

(a) Longitudinal velocity

(b) Lateral velocity

(c) Longitudinal acceleration

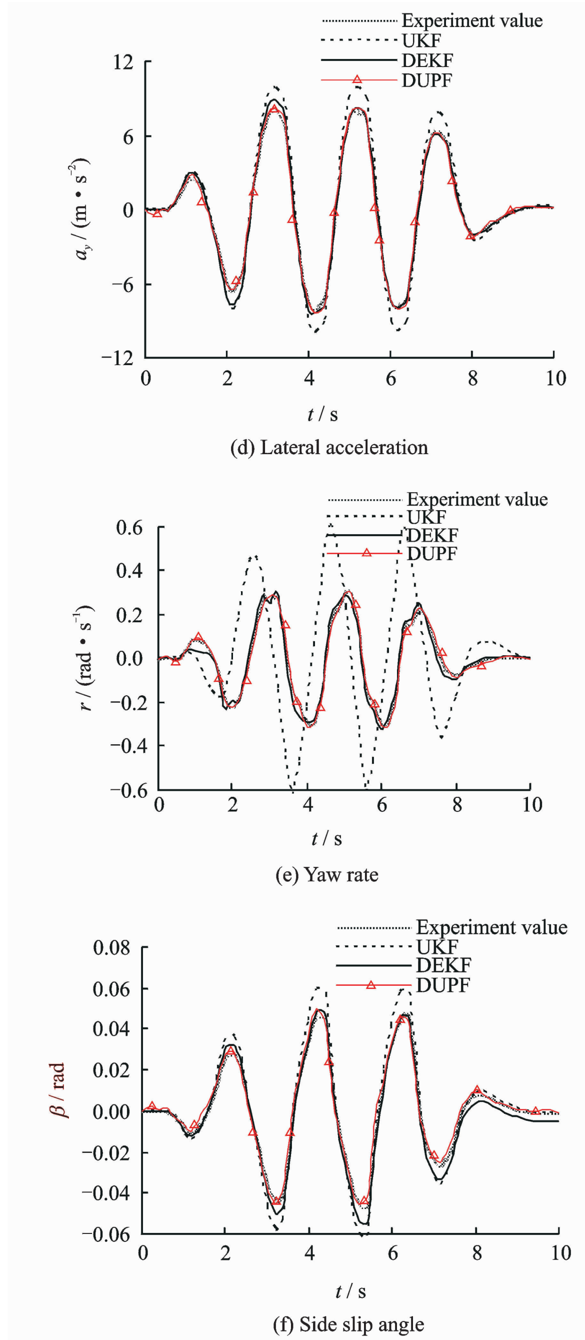

(d) Lateral acceleration

(e) Yaw rate

(f) Side slip angle

Fig. 4 Comparison between estimated and virtual experiment value

As shown in Fig. 4, the estimation accuracy of DUPF algorithm is higher than that of UKF and DEKF. Because UKF algorithm does not contain parameter estimator, the accuracy of UKF is apparently lower than that of DEKF and DUPF, even the values become seriously distorted in the estimation of yaw rate. The estimation error of each state in the wave crest and trough are higher than that in other places. It shows that the tires enter the nonlinear region at this moment. An improved tire model may improve the real-time performance of state estimation.

To have a quantitative comparison between the three algorithms, Table 1 gives the root mean square error (RMSE) and mean absolute error (MAE) of each algorithm.

Table 1 MAE and RMSE of each algorithm

Parameter		UKF	DEKF	DUPF
MAE	u	0.438	0.207	0.005 07
	v	0.196	0.089 7	0.070 5
	a_x	0.226	0.168	0.162
	a_y	0.768	0.343	0.154
	r	0.218	0.016 8	0.013 4
	β	0.008 64	0.003 64	0.001 97
RMSE	u	0.598	0.224	0.006 41
	v	0.283	0.106	0.094 3
	a_x	0.25	0.193	0.188
	a_y	1.12	0.617	0.215
	r	0.379	0.021 4	0.018 5
	β	0.010 9	0.006 39	0.002 62

As shown in Table 1, under the same circumstance, the estimation accuracy of DUPF is higher than that of the other two algorithms. In addition, the superiority of DUPF also lies in the algorithm itself: DEKF algorithm must solve complicated Jacobian matrix during estimation, which brings down the real-time property and increase the tendency of failure, while DUPF algorithm has not this defect.

In the DUPF algorithm, state estimation and parameter estimation run in parallel. To verify the parameter correction ability of this algorithm, Figs. 5—7 give the value of vehicle mass m, moment of inertia I_z and distance from center of mass to front akle a in the whole estimation process.

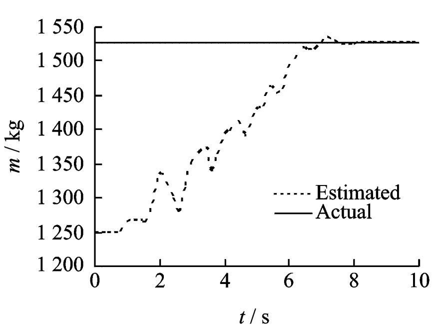

Fig. 5 Estimated and actual values of m

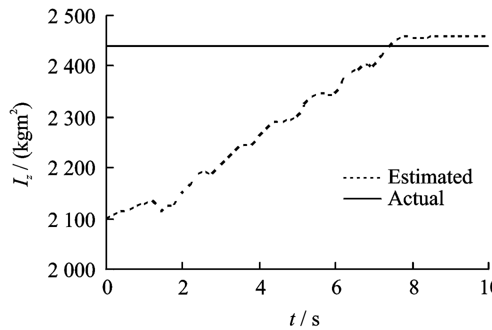

Fig. 6 Estimated and actual values of I_z

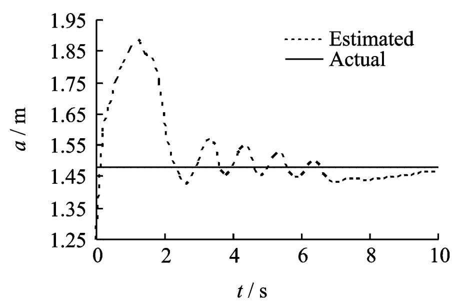

Fig. 7 Estimated and actual values of a

As shown in Figs. 5—7, the three estimated vehicle parameters tend to approach the true value alone with the time. This proves that DUPF has the ability to eliminate the influence from inaccurate parameters of the vehicle model, thus enables a state estimation based on relatively accurate vehicle model.

5 Proving Ground Test

For further testing the performance of DUPF, a full vehicle test is conducted on a light off-road vehicle in Serpentine Route. The test vehicle is equipped with gyroscopes to collect data of vehicle yaw rate and lateral acceleration in real-time. Non-contact speed sensors are also applied for gathering longitudinal and lateral velocity in real-time. In addition, ABS wheel speed sensors is used to gather angular velocity data of each tire and steering wheel angle sensor is used to gather steering wheel angle data. Vehicle test velocity is 65 km/h (±3 km/h). Figs. 8—10 give the comparison between the DUPF estimated and experimental value toward three key state parameters v, a_y, r.

As in the comparison above, though the esti-

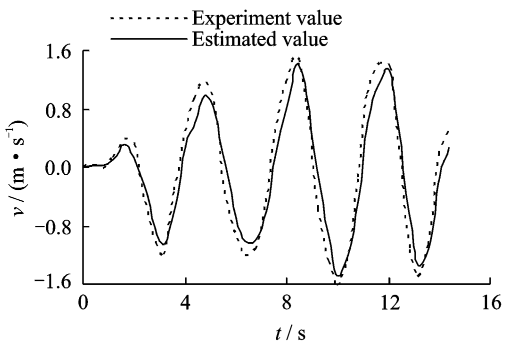

Fig. 8 Estimated and experimental values of v

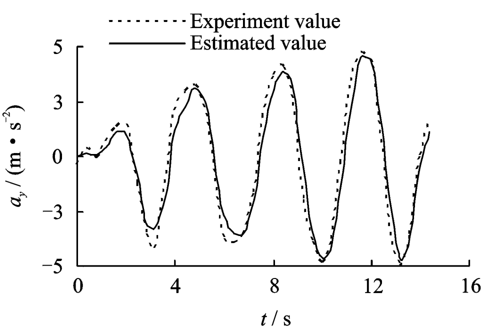

Fig. 9 Estimated and experimental values of a_y

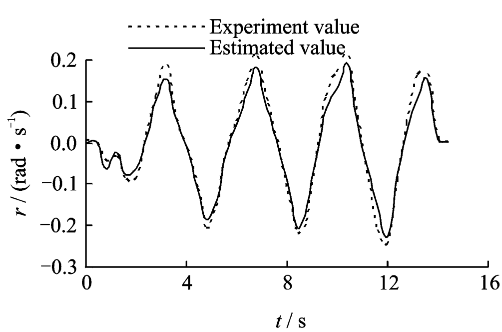

Fig. 10 Estimated and experimental values of r

mated value remains certain little errors, it generally accords with the experimental value. Historical values are used in the next step in discrete process, which causes the accumulation of error.

In addition, PAC 89 tire model still has error in simulating the vehicle tire mechanical property, moreover, sensor measurement error and sensor displacement are also main causes of error between the estimated and experimental value.

6 Conclusions

(1) This work proposed DUPF and applied it into the vehicle states and parameters estimation. The algorithm had two unscented particle filters run in parallel. States and parameters updated alternately. This algorithm is able to conduct states and parameters parallel estimation of a non-linear system containing inaccurate model parameters and constant noise.

(2) The DUPF algorithm adopted in this study demonstrates a well precision in state estimation towards non-linear vehicle system containing additive noise. Under the ADAMS high speed extreme driving condition, the mean absolute error of all the states are controlled fewer than 10% of the amplitude of each state, indicating that DUPF had satisfactory states estimation accuracy and parameter correction ability. Additionally, DUPF is completely competent for vehicle state estimator.

(3) The idea to integrate DUPF algorithm with vehicle key state parameter estimation can provide theoretical guide to the software design of the estimator in the vehicle automatic control system.

References:

[1] Ryu J H. State and parameter estimation for vehicle dynamics control using GPS[D]. California: Stanford University, 2005.

[2] Venhovens P J, Naab K. Vehicle dynamics estimation using Kalman filters[J]. Vehicle System Dynamics, 1999, 32(2): 171-184.

[3] Wenzel T A, Burnham K J, Blundell M V, et al. Kalman filter as a virtual sensor: Applied to automotive stability systems[J]. Transactions of the Institute of Measurement and Control, 2007, 29(2):95-115

[4] Best M C, Newton A P, Tuplin S. The identifying extended Kalman filter: Parametric system identification of a vehicle handling model[J]. Proc IMechE, Part K:Journal of Muti-body Dynamics, 2007, 211(1):87-98

[5] Dakhlallah J, Glaser S, Mammar S, et al. Tire-road forces estimation using extended Kalman filter and sideslip angle evaluation[C]//American Control Conference. Seattle, USA:IEEE,2008:4597-4602.

[6] Cheng Q, Correa-Victorino A, Charara A. A new

nonlinear observer using unscented Kalman filter to estimate sideslip angle, lateral tire road forces and tire road friction coefficient [C]//IEEE Intelligent Vehicles Symposium. Baden-Baden, Germany: IEEE, 2011:709-714.

[7] Wan E A, Nelson A T. Kalman filtering and neural networks [M]. New York: John Wiley & Sons, 2001

[8] Melzi S, Sabbioni E. On the vehicle sideslip angle estimation through neural networks: Numerical and experimental results[J]. Mechanical Systems and Signal Processing. 2011, 25(6): 2005-2019.

[9] Cherouat H, Braci M, Diop S. Vehicle velocity, side slip angles and yaw rate estimation[C]//IEEE International Symposium on Industrial Electronics. Dubrovnik, Croatia: IEEE, 2005:349-354.

[10] Shi Shuming, Lupker H, Bremmer P, et al. Estimation of vehicle side slip angle based on fuzzy logic[J]. Automotive Engineering, 2005, 27(4):426-430

[11] Kiencke U, Nielsen L. Automotive control systems [M]. Berlin: Springer, 2000.

[12] Bakker E, Pacejka H B, Lidner L. A new tire model with an application in vehicle dynamics studies. [EB/OL]. (1989-04-01)/[2013-10-31]. http://Papers.sae.org/8900871.

[13] Arulampalam M, Maskell S, Gordon N, et al. A tutorial on particle filters for online nonlinear/non-Gaussian Bayesian tracking[J]. IEEE Transactions on Signal Processing, 2002, 50(2):174-188.

(Executive editor: Zhang Bei)